Talanta 130 (2014) 39–48

Contents lists available at ScienceDirect

Talanta

journal homepage: www.elsevier.com/locate/talanta

Discrimination of micromass-induced chondrocytes from human mesenchymal stem cells by focal plane array-Fourier transform infrared microspectroscopy

Chirapond Chonanant [a,1], Keith R. Bambery [b,1], Nichada Jearanaikoon [c], Sirinart Chio-Srichan [c], Temduang Limpaiboon [d], Mark J. Tobin [b], Philip Heraud [e,f,*], Patcharee Jearanaikoon [d,**]

[a] Department of Medical Technology, Faculty of Allied Health Sciences, Burapha University, Chonburi 20131, Thailand
[b] Australian Synchrotron, Clayton, VIC 3800, Australia
[c] Synchrotron Light Research Institute, Public Organization, Nakhon Ratchasima 30000, Thailand
[d] Centre for Research and Development of Medical Diagnostic Laboratories, Faculty of Associated Medical Sciences, Khon Kaen University, Khon Kaen 40002, Thailand
[e] Centre for Biospectroscopy, School of Chemistry, Monash University, Clayton, VIC 3800, Australia
[f] Department of Anatomy and Developmental Biology, Monash University, Clayton, VIC 3800, Australia

ARTICLE INFO

Article history:
Received 24 February 2014
Received in revised form
19 May 2014
Accepted 20 May 2014
Available online 27 June 2014

Keywords:
Human mesenchymal stem cells
Micromass culture technique
Chondrogenic differentiation
FPA-FTIR microspectroscopy

ABSTRACT

Rapid and sensitive methods for identifying stem cell differentiation state are required for facilitating future stem cell therapies. We aimed to evaluate the capability of focal plane array-Fourier transform infrared (FPA-FTIR) microspectroscopy for characterising the differentiation of chondrocytes from human mesenchymal stem cells (hMSCs). Successful induction was validated by reverse transcription polymerase chain reaction (RT-PCR) and Western blot analysis for collagen and aggrecan expression as chondrocyte markers in parallel with the spectroscopy. Spectra derived from chondrocyte-induced cells revealed strong IR absorbance bands attributed to collagen near 1338 and 1234 cm^{-1} and proteoglycan at 1245 and 1175–960 cm^{-1} compared to the non-induced cells. In addition, spectra from control and induced cells are segregated into separate clusters in partial least squares discriminant analysis score plots at the very early stages of induction and discrimination of an independent set of validation spectra with 100% accuracy. The predominant bands responsible for this discrimination were associated with collagen and aggrecan protein concordant with those obtained from RT-PCR and Western blot techniques. Our findings support the capability of FPA-FTIR microspectroscopy as a label-free tool for stem cell characterization allowing rapid and sensitive detection of macromolecular changes during chondrogenic differentiation.

1. Introduction

Human mesenchymal stem cells (hMSCs) with multiple differentiation potentials are preferred as the predominant cell sources for cartilage tissue engineering [1]. To date, most of the standard protocols for determining stem cell differentiation are laborious and involve cell isolation, fixation and subsequent specific staining. Specialized expensive reagents, as well as stem cell samples, are consumed during multiple testing procedures. In addition, individual sample preparation can be evaluated for only one or two markers at a time. Taken together, these conventional methods are complicated and impractical for the routine analysis of differentiated MSCs destined to be used in clinical practice. Fourier transform infrared (FTIR) microspectroscopy offers the possibility to replace standard methods in stem cell studies. Indeed, previous work has demonstrated the ability of FTIR spectroscopy to detect cells differentiated from stem cells both in vitro [2] and in vivo [3]. As a labeled free technique, FTIR microspectroscopy allows the derivation of a biochemical fingerprint of macromolecules in the cell samples that variously absorb in the mid-IR spectral region. The unique characteristics of IR absorption bands are represented

* Corresponding author at: Centre for Biospectroscopy, School of Chemistry, Monash University, Clayton, VIC 3800, Australia. Tel./fax: +61 3 9905 4597.
** Corresponding author at: Centre for Research and Development of Medical Diagnostic Laboratories, Faculty of Associated Medical Sciences, Khon Kaen University, Khon Kaen, Kaen40002, Thailand. Tel./fax: +66 4334 7482.
E-mail addresses: phil.heraud@monash.edu (P. Heraud), patjea@kku.ac.th (P. Jearanaikoon).
[1] These two authors contributed equally to this work.

http://dx.doi.org/10.1016/j.talanta.2014.05.037
0039-9140/

for proteins (amide I band at ~1650 cm^{-1}; amide II at ~1545 cm^{-1}; and amide III at ~1300 cm^{-1}), lipid (CH stretching bands at 3000–2800 cm^{-1}; CO stretching from ester groups at ~1730 cm^{-1}) and nucleic acids (asymmetric PO_2^- stretching from nucleic acids at ~1240 cm^{-1}; symmetric PO_2^- stretching from nucleic acids at ~1080 cm^{-1}) [4]. Therefore, FTIR microspectroscopy enables the probing of differences or changes in cellular structures or states.

Although various cell culture methods such as pellet culture, monolayer culture and biomaterial-based scaffold culture have been developed, cell density of induced chondrocytes are still limited [5–9]. Pellet cultures are normally performed in 15 ml polypropylene conical tubes which occupy much incubator space. Change of medium in this system would also be laborious and costly. Furthermore, a number of published papers reported that a tightly aggregated pellet prepared by centrifugation often creates undifferentiated or necrotized cells in the central region of the pellet and only the peripheral cells underwent chondrogenic differentiation [10–14]. Thus, pellet culture is limited for use in clinical applications. Recently, the micromass culture system developed by Scharstuhl et al. [15] was demonstrated to be superior to the pellet culture system in terms of the yield of viable, differentiated cells. Moreover, the micromass system allows spontaneous cell aggregation, and the loose packing of cells compared with cell pellet culture improves diffusion of nutrients and growth factors. Accordingly, higher expression of chondrocyte markers was found in micromass culture compared to that in pellet cultures [12]. Hence, the micromass culture system exhibits more potential for chondrogenic induction.

Synchrotron sources enable an increase in sensitivity by generating more brilliant IR than conventional sources, allowing good signal-to-noise ratio (*S*/*N*) measurement at very small apertures, allowing the best spatial resolution to be achieved [16–19]. However, application of synchrotron-based FTIR microspectroscopy to biomedical research has been limited due to the restricted availability of synchrotron sources. The FTIR spectrometer coupled with a FPA detector operated in the so-called wide-field or global imaging mode is becoming more advantageous in terms of rapid data acquisition time and ease of use compared with synchrotron-based measurement systems. Indeed, the study by Heraud et al. [20] showed that FPA-FTIR microspectroscopy can produce a similar result to a synchrotron-based method when FPA images and synchrotron maps of biological tissue were compared. FPA-FTIR microspectroscopy has also been reported for characterization of various types of human cells and tissues, including brain [21], colon [22], cervix [23], lung [24] as well as stem cell study [4,25,26]. From a previous study, we clearly reported the capability of synchrotron radiation-FTIR to detect differentiation of chondrocyte-induced hMSCs. In this study, we evaluated for the first time the capability of FPA-FTIR microspectroscopy to discriminate the differentiation state of micromass-induced chondrocytes from hMSCs under growth factors (TGF-β3 and BMP-6) supplement for 7, 14 and 21 days. The changes observed in FTIR absorbance bands attributed to collagen (amide III band at 1338 cm^{-1} and the P–O stretching band at 1234 cm^{-1}) as well as proteoglycan (S–O stretching band at 1245 cm^{-1} and C–O–C stretching bands from carbohydrate at 1175–960 cm^{-1}) were used as indicators to monitor chondrocyte differentiation from hMSCs [17,27].

2. Experimental section

2.1. Chondrogenic induction using micromass culture

Human bone marrow mesenchymal stem cells (hBMSCs) purchased from Cambrex Bio Science, Walkerville, MD (cat no. PT-2501) were subjected to chondrogenic induction using micromass culture system, according to the protocol by Mello and Tuan [28]. In brief, hBMSCs were harvested and resuspended in Dulbecco's modified Eagle's medium with a low glucose concentration (DMEM-LG; Gibco Invitrogen) containing 100 U/ml penicillin, 100 μg/ml streptomycin (Gibco Invitrogen) and 10% fetal bovine serum (HyClone, Cramlington, UK) to achieve a final cell suspension of 4×10^6 cells ml^{-1}. To establish micromass cultures, 10 μl drops of cell suspension were spotted in each well of a 24-well plate. After spotting with cells, the plate was pre-incubated for 2 h at 37 °C to permit cell attachment, followed by addition of 300 μl of differentiation medium consisting of DMEM-high glucose with L-glutamine, sodium pyruvate, and pyridoxine hydrochloride (Gibco Invitrogen), 100 U/ml penicillin, 100 μg/ml streptomycin (Gibco Invitrogen), 50 μg/ml L-ascorbicacid-2-phosphate (Sigma-Aldrich, St Loius, MO), 0.4 mM L-proline (Sigma-Aldrich), 10^{-7} M dexamethasone (Sigma-Aldrich), 1% ITS+1 (Sigma-Aldrich), 250 ng/ml of BMP-6 (Sigma-Aldrich) and 10 ng/ml of TGF-β3 (Sigma-Aldrich). The medium was replaced every 3–4 days for 3 weeks. Control cells were cultured in parallel without additional growth factors. Three independent experiments were carried out to minimize the change in culture condition. Cells were collected at 7, 14 and 21 days for RNA and protein extraction (Fig. 1).

2.2. Detection of mRNA expression of chondrocyte markers by RT-PCR

Control and chondrocyte-induced cells at day 7, 14 and 21 were subjected to mRNA extraction using RNeasy mini kit (Qiagen, Hilden, Germany), based on the manufacturer's instructions. Approximately 1 μg of total RNA was then converted to cDNA. RT-PCR of three specific chondrocyte marker genes; collagen type II (*col II*), SRY (sex determining region *Y*)-box 9 (*SOX9*) and aggrecan (*AGC*) was performed to verify the successful induction of chondrogenesis. The amplification was carried out in a Thermal Cycler (Corbett Life Science, Australia). The following primers were used: *col II*: 5′-CAG AAG ACC TCA CGC CTC-3′, 5′-TAG TTT CCT GCC TCT GCC TTG AC-3′; *SOX9*: 5′-TGA AGA AGG AGA GCG AGG AG-3′, 5′-GCG GCT GGT ACT TGT AAT CC-3′; *AGC*: 5′-CAG GTG AAG ACT TTG TGG ACA TCC-3′, 5′-CCT CCT CAA AGG TCA GCG AGT AGC-3′; and Glyceraldehyde-3-phosphate dehydrogenase (*GAPDH*): 5′-GTC AGT GGT GGA CCT GAC CT-3′, 5′-AGG GGA GAT TCA GTG TGG TG-3′. The reaction mixture was incubated initially at 94 °C for 2 min, followed by 35 cycles of denaturation at 94 °C for 40 s, annealing at 54–60 °C for 40 s and extension at 72 °C for 60 s. The amplified product was separated by 2% agarose gel electrophoresis, stained with ethidium bromide and visualized under an UV trans-illuminator.

2.3. Detection of chondrocyte protein markers by Western blot analysis

Cells were collected at the indicated time points and lysed with 100 μl of protein extraction buffer containing 10 M Tris HCl pH 8.0, 2 M phenylmethanesulfonylfluoride (PMSF) and 1 × phosphatase inhibitor mixture (Roche, Mannheim, Germany). Lysates were incubated on ice for 30 min, homogenized, and centrifuged at 13,000 × *g* for 15 min. The supernatant was collected, and protein concentrations were determined by using the Lowry assay. Equal amounts of protein extracts (~30 μg) were fractionated by 7.5–12% SDS-PAGE and transferred onto PVDF membranes (Amersham Biosciences). Blots were probed at 4 °C overnight with mouse monoclonal anti-human collagen type II (Chemicon International, Temecula, USA) and mouse monoclonal anti-human cartilage proteoglycan (Chemicon International) at a dilution of

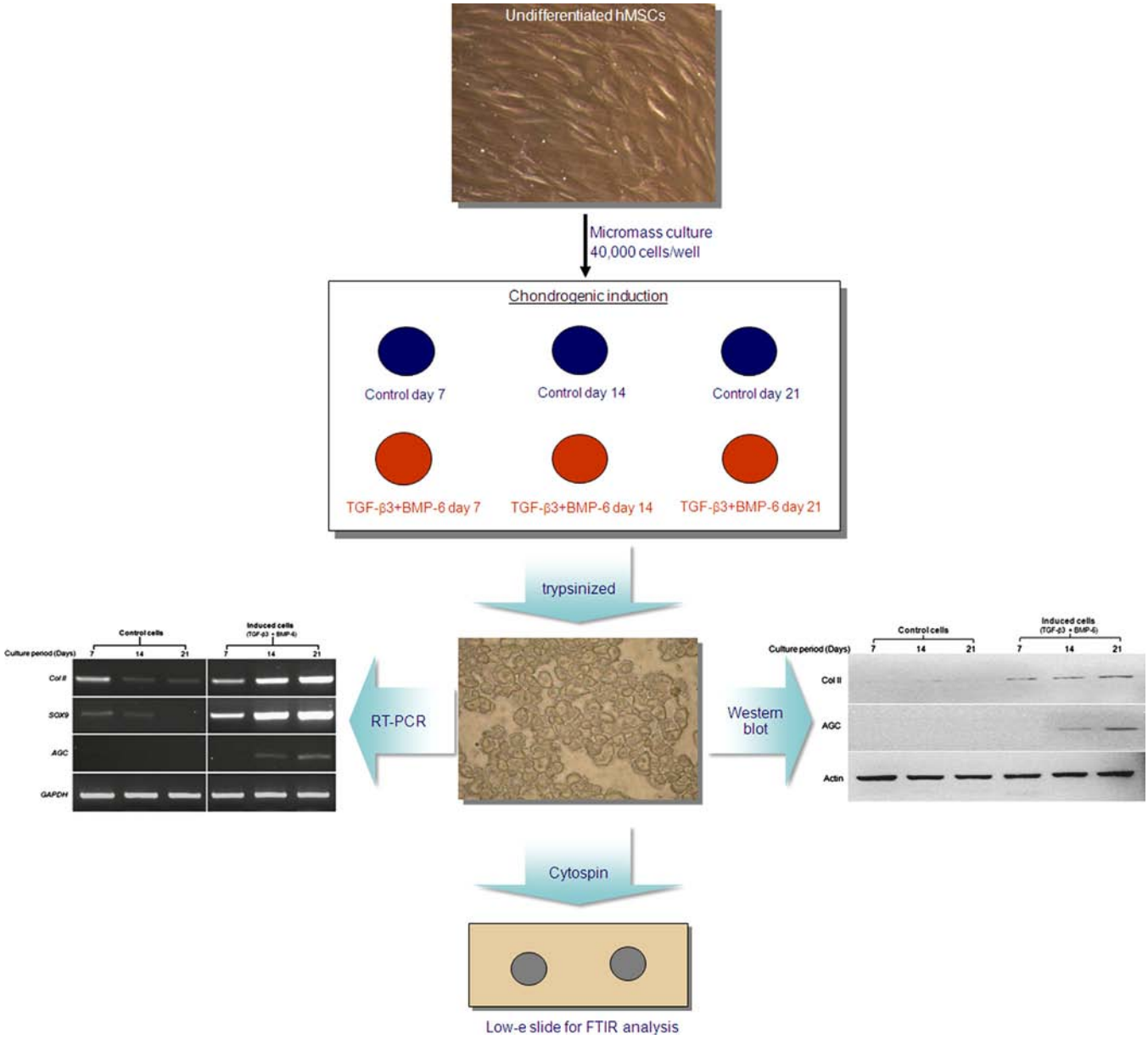

Fig. 1. Flow diagram illustrating the preparation of cells for FPA-FTIR microspectroscopic analysis of chondrocyte induction from hMSCs using the micromass culture technique.

1:50 as well as rabbit polyclonal anti-human β-Actin (Abcam, Cambridge, UK) diluted at 1:3000. The blots were subsequently incubated in horseradish peroxidase-conjugated secondary antibodies (anti-rabbit IgG, 1:3000, Abcam; or anti-mouse IgG, 1:3000, Abcam) at 37 °C for 1 h, immunoblotted using the ECL system (Amersham Biosciences), and visualized using the ImageQuant400 machine (Amersham Biosciences).

2.4. FTIR-FPA microspectroscopy

After 7, 14 and 21 day of differentiation, two replicate cultures of the control and induced samples were washed several times in PBS, trypsinized for 3 min then the cells were collected by centrifugation at $500 \times g$ for 5 min at 4 °C. The suspensions of undifferentiated or differentiated hMSCs were deposited on IR reflective, Low-e slides (Kevley Technologies, Chesterland, OH, USA) by a cyto-centrifuge (Cytospin III, Thermo Fischer Scientific, Waltham, MA) to produce a monolayer of cells on the surface of the slides and then dried under light vacuum in a desiccator prior to FTIR microspectroscopic analysis. This procedure involving cyto-centrifugation of cells and subsequent desiccation has been shown to result in cellular monolayers that are very consistent in thickness [29], hence minimising the possible effect of the electric field standing wave (EFSW) on the results [30].

Spectral data were collected on a Bruker Vertex 80V FTIR spectrometer attached to a Hyperion 2000 FTIR microscope (Bruker Optik GmbH, Ettlingen, Germany). The detector of the infrared microscope was liquid nitrogen cooled 64×64 pixel mercury cadmium telluride (MCT) FPA detector. FTIR spectra were acquired in transflection mode with 128 co-added scans at 8 cm^{-1} spectral resolution. Each image consisted of 1024 spectra from an area approximately 300 μm × 300 μm on the sample plane, with 4 adjacent pixels binned. The area of the sample from which single spectra were acquired was approximately 11 μm × 11 μm. Apodization was performed using a Happ–Genzel function. Acquisition was taken approximately 5 min per image.

2.5. Spectral imaging and multivariate data analysis

Spectra were pre-processed by applying resonant Mie scattering extended multiplicative signal correction (RMieS-EMSC) for removing the baseline distortions [31,32]. RMieS-EMSC was performed to 12 iterations starting with a baseline corrected average hBMSC spectrum as the reference spectrum. FTIR spectral images were constructed using CytoSpec™ (Cytospec Inc., Boston MA, USA) spectroscopic software. FTIR spectral images were constructed to show the distribution of two chondrocyte marker protein concentrations. Type II collagen concentration was estimated from the sulphate stretching band in the region 1255–1215 cm^{-1} [27,33], and aggrecan concentration was estimated from the area of the prominent band in induced samples resulting largely from glycoaminoglycan side chains in the spectral region from 1180 to 1140 cm^{-1} [27,33], using second derivative, vector-normalized spectra. The colour scheme in CytoSpec™ represents the concentration of those proteins with red colour indicating the strongest absorbance and blue for the lowest. Spectra processed using CytoSpec™ software allowed us to exclude spectra that obtained maximum absorbance less than 0.2 or greater than 0.8 absorbance units over the spectrum range of 950–1750 cm^{-1}, which eliminated spectra arising from regions devoid of cells or other areas where cells were clumped [17,34]. Based on this exclusion, approximately 150 spectra were obtained from each experimental group.

Prior to multivariate analyses or classification the obtained spectra were pre-processed by performing the second derivative using the Savitzky–Golay algorithm with 9 smoothing points, and normalization using EMSC [35]. The processing of spectra to the second derivative has been demonstrated to minimise the influence of the effects of EFSW on IR spectra acquired on transflection substrates [36]. The Unscrambler® 9.7 software (Camo Inc., Oslo, Norway) was used for multivariate data analysis.

Spectra acquired from control cells (undifferentiated hMSCs) and induced cells (cells undergoing chondrogenic induction from hMSCs) at each time point were randomly separated into calibration and validation sets, comprising approximately two-thirds and one-third of spectra, respectively. The calibration data matrix employed for PLS-DA consisted of the spectral dataset (multivariate X) and two Y variables with integer values of 0 or 1 coding for the each of the two modelled spectral classes. Classification of the dataset was then carried out by predicting a Y value for each spectrum in the independent validation using PLS models that had been generated from the calibration sets. Correct classification of each class was arbitrarily assigned to samples with predicted $Y > 0.5$ for respective spectra. PLS scores and regression loading plots were used to determine which spectral regions contributed most to the ability to classify spectra using PLS-DA.

3. Results and discussion

Human mesenchymal stem cells (hMSCs) were differentiated toward chondrocytes in serum-free medium supplemented with TGF-β3 and BMP-6 over a period of 7, 14 and 21 days of induction. After 24 h of supplementation with growth factors, the cell droplets spontaneously aggregated and became spherical compared to the

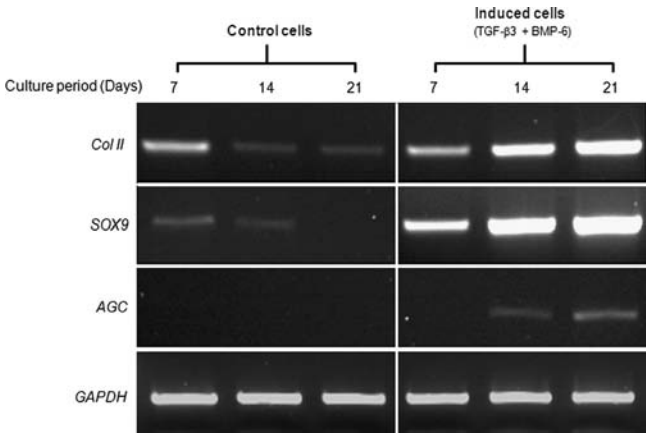

Fig. 3. RT-PCR analysis of *col II*, *SOX9* and *AGC* expression during chondrogenesis induced by TGF-β3 and BMP-6 for 7, 14 and 21 days using the micromass culture system. Chondrogenic gene expression was unregulated in the induced cells compared to the control cells. Glyceraldehyde-3-phosphate dehydrogenase (*GAPDH*) was used as a control.

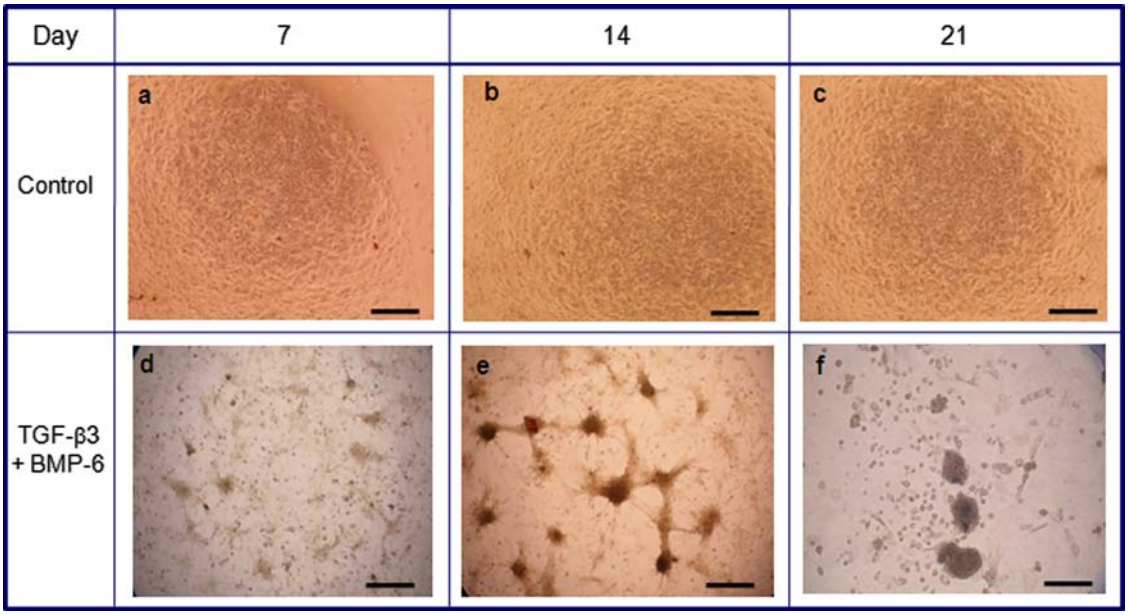

Fig. 2. Micromass culture system was performed to induce chondrogenesis from hMSCs over a period of 7, 14 and 21 days of induction. After growth factors supplementation, the cell droplets spontaneously aggregated and became spherical when compared to control cells. Scale bar = 200 μm.

control cells (data not shown). An increase in size of the aggregated micromass cells was observed through the period of induction (Fig. 2) indicating that the micromass culture system can permit a three dimensional environment that allowed cell–cell interactions similar to those observed in pre-cartilage condensations found during embryonic development [12].

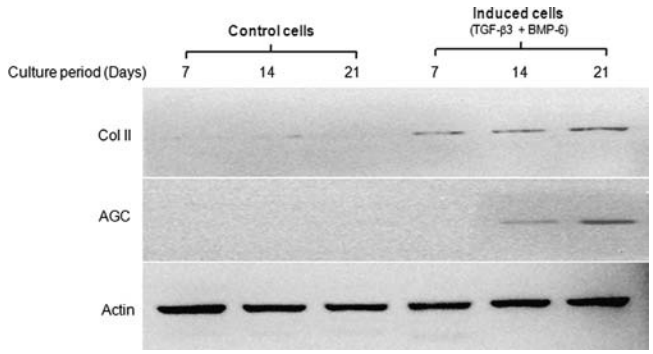

Fig. 4. Western blots illustrating chondrocyte marker proteins in response to TGF-β3 and BMP-6 at the indicated time-points. The levels of type II collagen and aggrecan in induced cells increased throughout the entire time period, this observation is consistent with the RT-PCR results. β-actin proteins were used as a control.

The chondrogenic induction was monitored by detection of the mRNA and protein expression of specific chondrocyte markers, *col II*, *SOX9* and *AGC* using RT-PCR (Fig. 3) and Western blot analysis (Fig. 4). The mRNA and protein expression of chondrocyte markers increased markedly from day 7 through day 21 under growth factor supplementation compared to controls. Although a minor background mRNA expression of *col II* and *SOX9* was detected in the control day 7, no protein band was observed on Western blot. This might have resulted from the residual serum contained in the expansion medium prior to replacement by serum free medium, which inherently obtained various inducible growth factors including insulin [37] that have been previously reported as chondrogenic stimulators [38,39]. Thus, these data indicated the successful induction of chondrogenic differentiation in hMSCs. To characterize the IR absorption pattern of chondrocyte markers, average spectra were calculated from the second derivative spectra over the range 1800 to 950 cm^{-1}, comparing between control (blue line) and chondrocyte-induced hMSCs (red line) at day 21 as shown in Fig. 5. The average spectra showed absorbance differences for the amide III bands near 1338 and 1234 cm^{-1} which were assigned to collagen, as well as bands at 1245 (S–O stretching) and 1175–960 (C–O–C stretching) cm^{-1} correlated with proteoglycan [27]. Accordingly, the absorbance of collagen at 1338 and 1234 cm^{-1} and aggrecan bands observed at 1245 cm^{-1}, 1165, 1080 and

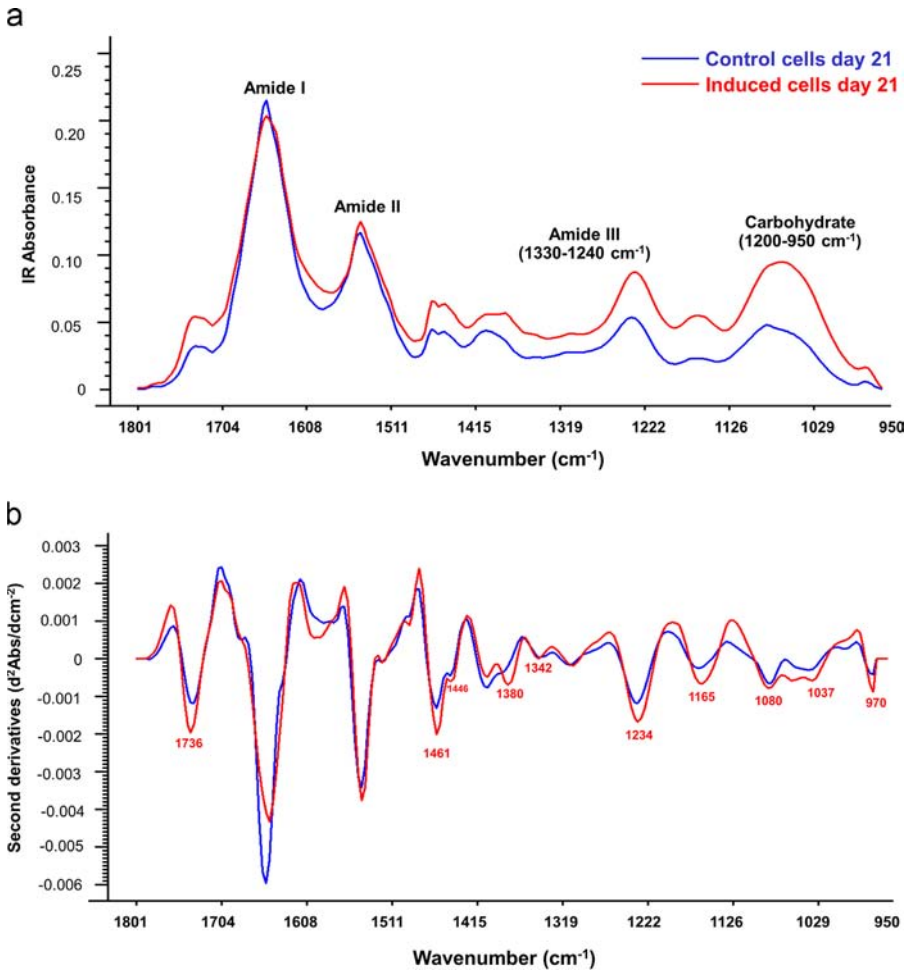

Fig. 5. Analysis of spectra from control and induced cells used FPA-FTIR microspectroscopy. (a) The representative average raw spectra from control (blue) and induced (red) cells day 21, after normalization and baseline correction over the range 1800–950 cm^{-1}. (b) To better resolve peaks that were overlapping in the raw spectra, the spectra were converted to second derivative spectra, which differed between induced and control samples mainly between 1330 and 950 cm^{-1}; these included the amide III absorbance band from proteins (1330–1230 cm^{-1}) and the carbohydrate absorbance region (1200–950 cm^{-1}). There was also an increase in lipid absorbance (bands from the lipid ester carbonyl stretching mode at ~1736 cm^{-1} and C–H bending mode at 1461 cm^{-1}). (For interpretation of the references to color in this figure legend, the reader is referred to the web version of this article.)

1037 cm^{-1} were higher in chondrocyte-induced hMSCs than those of control samples. These results are well correlated with the RT-PCR and Western blot techniques.

The concentration and distribution of chondrocyte markers were illustrated by chemical images of collagen and aggrecan in Fig. 6. The comparison between chemical imaging of control and induced samples at day 21 (Fig. 6a) were analyzed using the spectral region between 1255 and 1215 cm^{-1} for collagen, while the chemical imaging of aggrecan was derived from the spectral region between 1180 and 1140 cm^{-1} as shown in Fig. 6b. The chemical images show the increase of concentration distribution of these two proteins in chondrocyte induced cells at day 21 compared to that in control cells.

Also evident from the average spectra (Fig. 5) and PCA loadings (Supplementary Fig.) are increases in lipid absorbance during the chondrogenic differentiation including bands at ~1460 cm^{-1} (anti-symmetric methyl and methylene bending) and ~1735 cm^{-1} (ester carbonyl stretching mode). An increase in lipid fatty acids during chondrogenesis has recently been reported in the literature [40]. The reason for increases in cellular lipid components during chondrogenesis was related by Jang et al. [40] was related to an upregulation of membrane lipids but is still not fully explained. Nevertheless, our data shows that increases in lipid signatures are clearly registered in the spectra of the differentiating cells and appears to be another unequivocal marker of chondrogenic differentiation along with the changes in aggrecan and collagen signatures discussed above.

PLS-DA scores and loadings plots were examined to determine the spectral features that enabled discrimination of FTIR spectra from induced and control samples at every time interval of the experiment. Scores plots showed distinct clustering of spectra from control samples (represented as blue points) and induced samples (represented as red points) at day 7 visualized along factor 1 (Fig. 7a). Control samples from day 14 and 21 of the induction periods were clustered separately from the induced samples along factor 1 (Fig. 7b and c, respectively). The separation between clusters of undifferentiated and differentiated cell spectra was more clearly defined when the time period of chondrogenic induction continued for 21 days.

PLS-DA regression loadings plots enabled identification of bands in the complex FTIR spectra which were responsible for the largest inter-spectral variance [41]. The regression loadings of controls versus induced samples from day 7, 14 and 21 cultures, shown in Fig. 7d–f, respectively, identified the bands that differed between control and induced cells (listed in Table 1). Significant loadings for all samples were found near 1338 and 1245 cm^{-1} attributed to collagen type II and aggrecan [27] and the spectral region between 1175 and 950 cm^{-1} attributed to C–O stretching vibrations from aggrecan [27,42–44]. These loadings corresponded to the band positions for the two proteins observed in the average second derivative spectra in Fig. 5b. These results are similar to those from our previous study using synchrotron-based FTIR [17,20], demonstrating that undifferentiated MSCs and

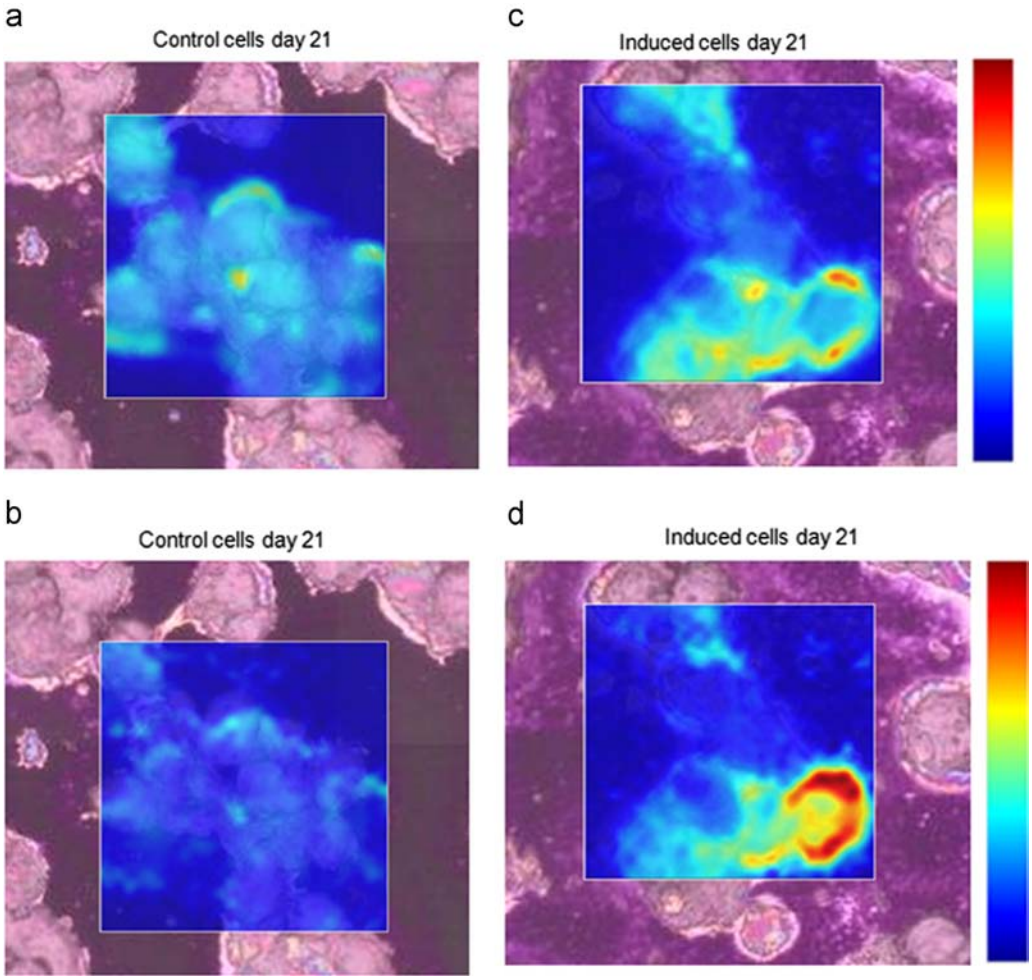

Fig. 6. A comparison between chemical imaging of control hMSCs and induced samples at day 21 for collagen (a) using the amide III band from collagen in the spectral region from 1255 to 1215 cm^{-1} and the C–O stretching band from aggrecan (b) at the region between 1180 and 1140 cm^{-1} in vector normalised, second derivative spectra. A colour scheme has been used to denote relative absorbances, with the warmest colours (red end of the spectrum) indicating the highest absorbance. Scale bar = 100 μm. (For interpretation of the references to color in this figure legend, the reader is referred to the web version of this article.)

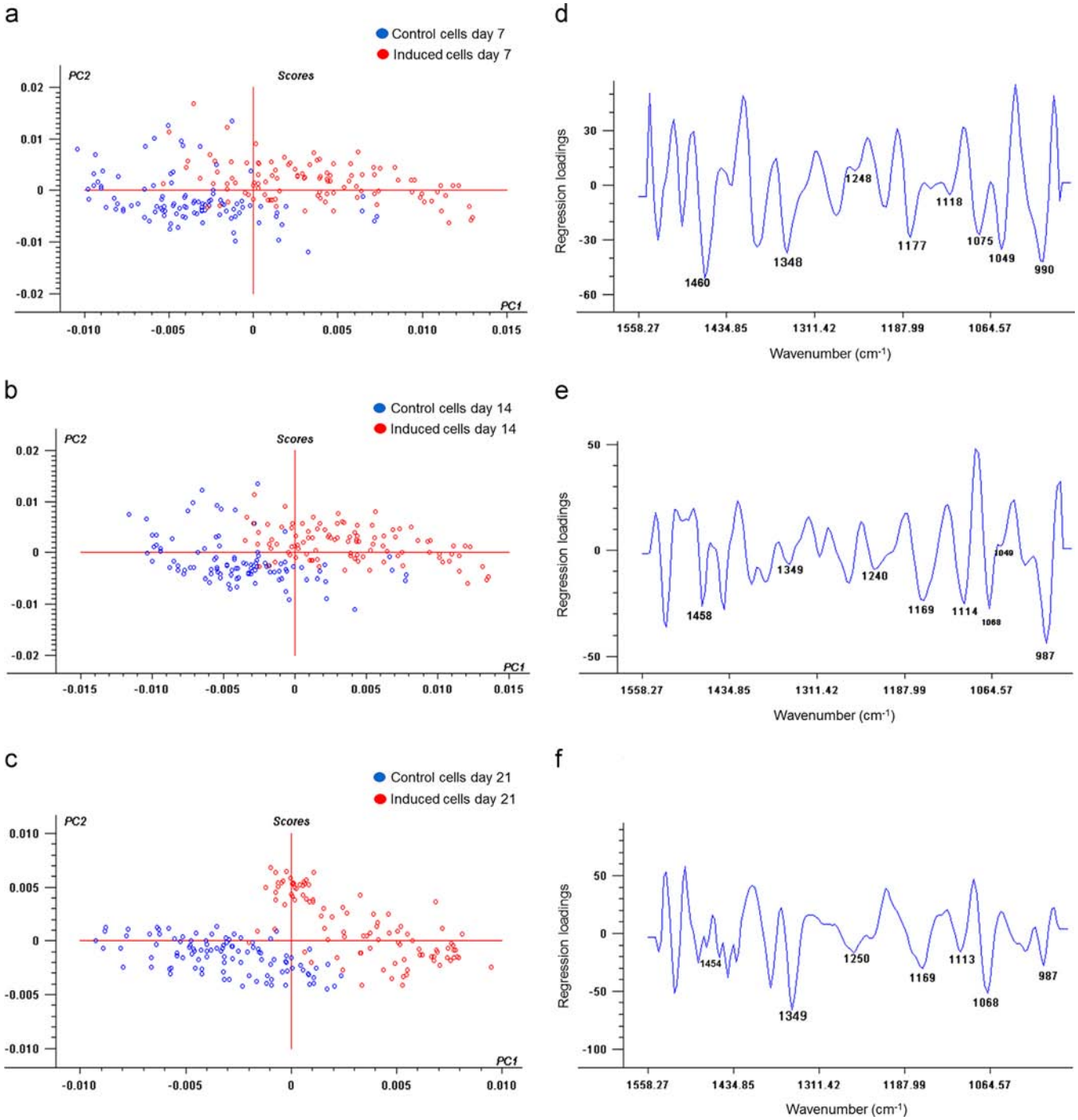

Fig. 7. PLS scores (a)–(c) and loadings (d)–(f) plots performed on a data set of control and induced cells at day 7 (a) and (d), day 14 (b) and (e) and day 21 (c) and (f) using the spectral range 1585–950 cm^{-1}. Corresponding loadings plots from all experiments showed a trend of similar spectral regions exhibiting the most variance attributable to changes in collagen and aggrecans (d)–(f). Six factors were computed in PLS DA. The percentage of variance captured found with factor 1 to factor 6 factor at day 7 are 42.016, 56.291, 74.245, 80.982, 84.835 and 87.244; at day 14 are 40.014, 65.045, 89.594, 90.663, 92.342 and 92.747; at day 21 are 53.460, 79.516, 89.346, 93.406, 93.774 and 94.722. (For interpretation of the references to color in this figure legend, the reader is referred to the web version of this article.)

differentiated progeny cells could be readily separated by their FTIR absorption profiles of chondrocyte marker proteins and carbohydrates. These observations were reproducible with three independent experiments. Furthermore, FPA-FTIR, RT-PCR and Western blot showed consistent differences between hMSCs and their differentiated progeny cells. In addition the similar pattern of separation is observed using PCA analysis as shown in supplemental table (Fig. S1).

PLS-DA modeling [45] allowed Y values from independent validation spectra to be predicted. To do this, Y values of control spectra at day 7, 14 and 21, samples were assigned $Y=0$ while spectra from induced samples at day 7, 14 and 21 were assigned $Y=1$. Spectral data were randomly divided into calibration and validation sets comprising two-thirds and one-third of spectra, respectively. A regression plot of the calibration data set for day 7 yielded a correlation coefficient=0.89 (Fig. 8a), day 14=0.93 (Fig. 8b), and day 21=0.94 (Fig. 8c), indicating that the calibration data set was well modeled. The Y values were then predicted for each spectrum in validation sets of spectra with correctly assigned control spectra having predicted $Y<0.5$ and correctly assigned

Table 1
Assignment of biological bands for the IR spectrum to chemical functional groups. Table of band assignments for the average spectra shown in Fig. 5b compared with the associated factor 1 regression coefficient loadings from Fig. 8. Arrows for factor 1 loadings (day 7) indicate up-or down-regulation of the macromolecular components related to the FTIR bands that differed between control cells at day 7 and induced cells at day 7 shown in scores plots in Fig. 8a as clustering in the factor 1 direction. Arrows for factor 1 loadings (day 14) indicate up regulation of the macromolecular components inferred to be changing between control cells at day 14 and induced cells at day 14 shown in scores plots in Fig. 8b as clustering in the factor 1 direction. Factor 1 loadings (day 21) indicate inferred macromolecular changes occurring between control samples at day 21 which separated from induced cells at day 21 along factor 1 in scores plots in Fig. 8c. The positive (+) or negative (−) signs represent the regression coefficient loadings value which were obtained from PLS discriminant analysis of second derivative spectra.

Bands maxima 2nd derivative spectra (cm^{-1})	Factor 1 loadings (day 7) (cm^{-1})	Factor1 loadings (day 14) (cm^{-1})	Factor 1 loadings (day 21) (cm^{-1})	Band assignments
1338	↑ 1348 (−)	↑ 1349 (−)	↑ 1349 (−)	ν(C–H) and δ(N–H) of amide III from protein [46]
1245	↑ 1248 (−)	↑ 1240 (−)	↑ 1250 (−)	ν(C–H) and δ(N–H) of amide III from protein [27] and ν_{as}(S=O) sulfate from glycoaminoglycan side chain of aggrecan [27,33]
1200–900	↑ 1177 (−)	↑ 1169 (−)	↑ 1169 (−)	ν(C–O–C) from aggrecan and other carbohydrates [27,43,44]
	↑ 1118 (−)	↑ 1114 (−)	↑1113 (−)	
	↑ 1075 (−)	↑ 1068 (−)	↑ 1068 (−)	
	↑ 1049 (−)	↑ 1049 (−)	↑ 987 (−)	
	↑ 990 (−)	↑ 987 (−)		

ν_{as}, asymmetric stretch; ν_s, symmetric stretch; δ_{as}, asymmetric deformation (bend); δ_s, symmetric deformation (bend).

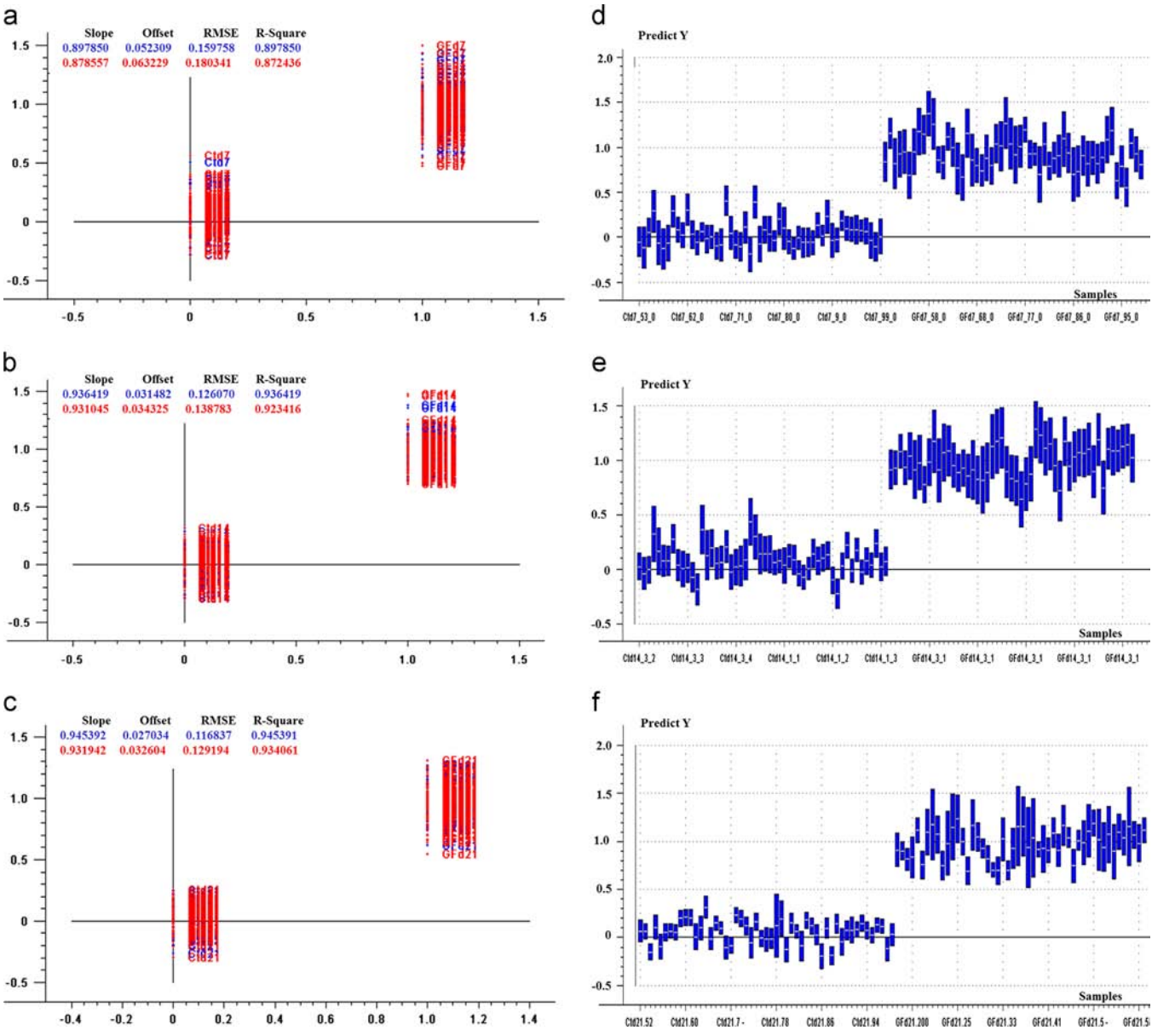

Fig. 8. PLS regression plot for the calibration set, which plotted measured *Y* against predicted *Y*. The correlation coefficients of day 7, 14 and 21 (a)–(c), respectively) indicated that the training set was well modeled. Predicted *Y* values shown as narrow blue rectangles, indicated that all validation spectra from all time points were correctly classified (d)–(f). (For interpretation of the references to color in this figure legend, the reader is referred to the web version of this article.)

induced samples spectra having predicted $Y > 0.5$. 100% of spectra from independent validation sets were correctly classified into each of the assigned classes of control and induced cells at day 7, 14 and 21 as shown in Fig. 8d–f, respectively.

Our data adds to the growing literature demonstrating capabilities of FPA-FTIR microspectroscopy for stem cell research. For example, the study by Krafft et al. [26] reported changes in protein composition and expression of octacalcium phosphate, a precursor of the bone constituent hydroxyapatite, during osteogenesis from hMSCs. A study on neural differentiation of mouse ESCs [25] using FPA-FTIR microspectroscopy found major changes in lipids and protein composition occurring during stem cell differentiation along neural lineages. Further supporting the view that FPA-FTIR microspectroscopy is a useful modality for studying stem cell differentiation, the study by Heraud et al. [4] investigated undifferentiated human ESCs and cells that had committed to mesendoderm or ectoderm lineages by a specific stimulus, demonstrating that FPA-FTIR microspectroscopy could characterize and discriminate hESCs from ectodermal and mesendodermal lineages by their specific infrared signatures, even at the very early stages of development.

The results presented here supported the view that FPA-FTIR microspectroscopy could identify the differences between hMSCs and chondrocyte-induced hMSCs, corroborating the changes of collagen and aggrecan identified by chemical imaging. Interestingly, the spectral quality generated by the FPA system enabled data that was comparable to that from a synchrotron source as previously reported [17,20], leading to similar conclusions about the macromolecular changes occurring as a result of chondrogenic induction. However, the FPA-FTIR microspectroscopy allowed much more rapid measurement compared with single point measurements using a synchrotron source enabling thousands of spectra to be obtained in a few minutes. Accordingly, we concluded that standalone FPA-FTIR microspectroscopy permitted rapid and easy detection of the differentiation state of chondrocytic cells as well as providing rapid evaluation of different stem cell culturing methods that were compared.

4. Conclusion

FPA-FTIR microspectroscopy can be used to characterize the changes in composition and distribution of collagen and aggrecan in chondrocyte-induced hMSCs. Our findings underscore the potential of FPA-FTIR methods to be used as a monitoring tool for identifying the successful differentiation of chodrocytes in both quality and quantity. In combination with chemometric methods, the spectroscopic approach provides high accuracy and sensitivity to detect an early differentiation state of stem cells. Future development of automated systems based upon FPA-FTIR microspectroscopy might represent a routine method of screening for identification of differentiated cells facilitating clinical applications.

Conflict of interest disclosure

The authors declare no competing financial interest.

Acknowledgement

This research was financially supported by a Strategic Scholarships for Frontier Research Network grant from the Office of the Higher Education Commission, Thailand and Synchrotron Light Research Institute (2551/04) (Public Organization), Thailand. The authors also acknowledge assistance and support provided by Monash Immunology and Stem Cell Laboratories, Monash University, Victoria, Australia, the Australian Synchrotron, Victoria, Australia and the Centre for Research and Development of Medical Diagnostic Laboratories, the Faculty of Associated Medical Sciences, Khon Kaen University, Khon Kaen, Thailand. This work was supported by the Multi-modal Australian ScienceS Imaging and Visualisation Environment (MASSIVE) (www.massive.org.au).

Appendix A. Supplementary material

Supplementary data associated with this article can be found in the online version at http://dx.doi.org/10.1016/j.talanta.2014.05.037.

References

[1] M.F. Pittenger, A.M. Mackay, S.C. Beck, R.K. Jaiswal, R. Douglas, J.D. Mosca, M.A. Moorman, D.W. Simonetti, S. Craig, D.R. Marshak, Science 284 (1999) 143–147.
[2] P. Heraud, E.S. Ng, S. Caine, Q.C. Yu, C. Hirst, R. Mayberry, A. Bruce, B.R. Wood, D. McNaughton, E.G. Stanley, A.G. Elefanty, Stem Cell Res. 4 (2010) 140–147.
[3] M.J. Walsh, A. Hammiche, T.G. Fellous, J.M. Nicholson, M. Cotte, J. Susini, N.J. Fullwood, P.L. Martin-Hirsch, M.R. Alison, F.L. Martin, Stem Cell Res. 3 (2009) 15–27.
[4] P. Heraud, E.S. Ng, S. Caine, Q.C. Yu, C. Hirst, R. Mayberry, A. Bruce, B.R. Wood, D. McNaughton, E.G. Stanley, A.G. Elefanty, Stem Cell Res. 4 (2010) 140–147.
[5] F. Djouad, D. Mrugala, D. Noel, C. Jorgensen, Regen. Med. 1 (2006) 529–537.
[6] T. Furumatsu, M. Tsuda, N. Taniguchi, Y. Tajima, H. Asahara, J. Biol. Chem. 280 (2005) 8343–8350.
[7] T. Ito, R. Sawada, Y. Fujiwara, T. Tsuchiya, Cytotechnology 56 (2008) 1–7.
[8] S. Zhou, K. Eid, J. Glowacki, J. Bone Miner. Res. 19 (2004) 463–470.
[9] R. Tuli, S. Tuli, S. Nandi, X. Huang, P.A. Manner, W.J. Hozack, K.G. Danielson, D.J. Hall, R.S. Tuan, J. Biol. Chem. 278 (2003) 41227–41236.
[10] A.D. Murdoch, L.M. Grady, M.P. Ablett, T. Katopodi, R.S. Meadows, T.E. Hardingham, Stem Cells 25 (2007) 2786–2796.
[11] W. Kafienah, S. Mistry, S.C. Dickinson, T.J. Sims, I. Learmonth, A.P. Hollander, Arthritis Rheum. 56 (2007) 177–187.
[12] L. Zhang, P. Su, C. Xu, J. Yang, W. Yu, D. Huang, Biotechnol. Lett. 32 (2010) 1339–1346.
[13] M.B. Mueller, R.S. Tuan, Arthritis Rheum. 58 (2008) 1377–1388.
[14] R.S. Tare, D. Howard, J.C. Pound, H.I. Roach, R.O. Oreffo, Biochem. Biophys. Res. Commun. 333 (2005) 609–621.
[15] A. Scharstuhl, B. Schewe, K. Benz, C. Gaissmaier, H.J. Buhring, R. Stoop, Stem Cells 25 (2007) 3244–3251.
[16] F. Le Naour, M.P. Bralet, D. Debois, C. Sandt, C. Guettier, P. Dumas, A. Brunelle, O. Laprevote, PLoS One 4 (2009) e7408.
[17] C. Chonanant, N. Jearanaikoon, C. Leelayuwat, T. Limpaiboon, M.J. Tobin, P. Jearanaikoon, P. Heraud, Analyst 136 (2011) 2542–2551.
[18] J.G. Kelly, T. Nakamura, S. Kinoshita, N.J. Fullwood, F.L. Martin, Analyst 135 (2010) 3120–3125.
[19] K. Thumanu, W. Tanthanuch, D. Ye, A. Sangmalee, C. Lorthongpanich, R. Parnpai, P. Heraud, J. Biomed. Opt. 16 (2011) 057005.
[20] P. Heraud, S. Caine, G. Sanson, R. Gleadow, B.R. Wood, D. McNaughton, New Phytol. 173 (2007) 216–225.
[21] C. Krafft, L. Shapoval, S.B. Sobottka, K.D. Geiger, G. Schackert, R. Salzer, Biochim. Biophys. Acta 1758 (2006) 883–891.
[22] C. Krafft, D. Codrich, G. Pelizzo, V. Sergo, J. Biophotonics 1 (2008) 154–169.
[23] W. Steller, J. Einenkel, L.C. Horn, U.D. Braumann, H. Binder, R. Salzer, C. Krafft, Anal. Bioanal. Chem. 384 (2006) 145–154.
[24] C. Krafft, D. Codrich, G. Pelizzo, V. Sergo, Vib. Spectrosc. 46 (2008) 141–149.
[25] W. Tanthanuch, K. Thumanu, C. Lorthongpanich, R. Parnpai, P. Heraud, J. Mol. Struct. 967 (2010) 189–195.
[26] C. Krafft, R. Salzer, S. Seitz, C. Ern, M. Schieker, Analyst 132 (2007) 647–653.
[27] N.P. Camacho, P. West, P.A. Torzilli, R. Mendelsohn, Biopolymers 62 (2001) 1–8.
[28] M.A. Mello, R.S. Tuan, in vitro Cell. Dev. Biol. Anim. 35 (1999) 262–269.
[29] J. Cao, E.S. Ng, D. McNaughton, E.G. Stanley, A.G. Elefanty, M.J. Tobin, P. Heraud, Analyst 138 (2013) 4147–4160.
[30] P. Bassan, J. Lee, A. Sachdeva, J. Pissardini, K.M. Dorling, J.S. Fletcher, A. Henderson, P. Gardner, Analyst 138 (2013) 144–157.
[31] P. Bassan, A. Kohler, H. Martens, J. Lee, H.J. Byrne, P. Dumas, E. Gazi, M. Brown, N. Clarke, P. Gardner, Analyst 135 (2010) 268–277.
[32] K.R. Bambery, B.R. Wood, D. McNaughton, Analyst 137 (2012) 126–132.
[33] K. Potter, L.H. Kidder, I.W. Levin, E.N. Lewis, R.G. Spencer, Arthritis Rheum. 44 (2001) 846–855.
[34] P. Heraud, B. Wood, J. Beardall, D. McNaughton, J. Chemometrics 20 (2006) 193–197.
[35] H. Martens, J.P. Nielsen, S.B. Engelsen, Anal. Chem. 75 (2003) 394–404.
[36] M. Miljkovic, B. Bird, K. Lenau, A.I. Mazur, M. Diem, Analyst 138 (2013) 3975–3982.

[37] J. van der Valk, D. Brunner, K. De Smet, Å. Fex Svenningsen, P. Honegger, L.E. Knudsen, T. Lindl, J. Noraberg, A. Price, M.L. Scarino, G. Gstraunthaler, Toxicol. in vitro 24 (2010) 1053–1063.
[38] T. Atsumi, Y. Ikawa, Y. Miwa, K. Kimata, Cell Differ. Dev. 30 (1990) 109–116.
[39] K. Hidaka, T. Kanematsu, H. Takeuchi, M. Nakata, U. Kikkawa, M. Hirata, Int. J. Biochem. Cell Biol. 33 (2001) 1094–1103.
[40] M.Y. Jang, S.I. Chun, C.W. Mun, K.S. Hong, J.W. Shin, PLoS One 8 (2013) e78325.
[41] M.J. Walsh, M.N. Singh, H.M. Pollock, L.J. Cooper, M.J. German, H.F. Stringfellow, N.J. Fullwood, E. Paraskevaidis, P.L. Martin-Hirsch, F.L. Martin, Biochem. Biophys. Res. Commun. 352 (2007) 213–219.
[42] J.J. Cael, J.L. Koenig, J. Blackwell, Carbohydr. Res. 29 (1973) 123–134.
[43] P.T. Wong, R.K. Wong, T.A. Caputo, T.A. Godwin, B. Rigas, Proc. Nat. Acad. Sci. U.S.A. 88 (1991) 10988–10992.
[44] W. Zeroual, C. Choisy, S.M. Doglia, H. Bobichon, J.F. Angiboust, M. Manfait, Biochim. Biophys. Acta 1222 (1994) 171–178.
[45] P. Geladi, J. Chemom. 2 (1988) 231–246.
[46] J. Bandekar, Biochim. Biophys. Acta 1120 (1992) 123–143.